Nationaal Lucht- en Ruimtevaartlaboratorium
National Aerospace Laboratory NLR

NLR TP 97151

Separation in transonic flow: a shocking experience

A. Elsenaar

DOCUMENT CONTROL SHEET

	ORIGINATOR'S REF.		SECURITY CLASS.
	NLR TP 97151 U		Unclassified

ORIGINATOR
National Aerospace Laboratory NLR, Amsterdam, The Netherlands

TITLE
Separation in transonic flow: a shocking experience

PRESENTED AT
the Seminar "Boundary-Layer Separation in Aircraft Aerodynamics" at the special occasion of the retirement of Prof. J.L. van Ingen, February 6, 1997 at the Technical University of Delft

AUTHORS	DATE	pp	ref
A. Elsenaar	970404	24	19

DESCRIPTORS

Boundary layer separation	Reynolds number
Boundary layer flow	Shockwave interaction
Delta wings	Transonic flow
Flow visualization	Turbulent boundary layer
Leading edges	Vortex breakdown
Pressure distribution	Windtunnel tests

ABSTRACT
The understanding of shock induced separation is of great practical importance for the design of aircraft. Early examples of shock induced separation are used to explain some of its characteristics. Empirical correlations show the main parameters involved. Based on this a better understanding of Reynolds number effects in transonic flow is obtained, including the possibility to "manipulate" the boundary layer separation such that high Reynolds number flow can be simulated at (lower) tunnel Reynolds numbers. Shock induced separation is also an important phenomenon for delta wing flows. When the free stream Mach number is sufficiently high, separation at the (rounded) wing leading edge will be shock induced and the cause of vortical flow over the wing. Under the vortex a secondary shock induced separation can be observed. Annd at high angles of attack and Mach numbers around 0.8 and above, vortex breakdown shows some aspects similar to shock induced separation. These examples illustrate the importance of shock induced separation at transonic conditions.

Abstract

The understanding of shock induced separation is of great practical importance for the design of aircraft. Early examples of shock induced separation are used to explain some of its characteristics. Empirical correlations show the main parameters involved. Based on this a better understanding of Reynolds number effects in transonic flow is obtained, including the possibility to "manipulate" the boundary layer separation such that high Reynolds number flow can be simulated at (lower) tunnel Reynolds numbers. Shock induced separation is also an important phenomenon for delta wing flows. When the free stream Mach number is sufficiently high, separation at the (rounded) wing leading edge will be shock induced and the cause of vortical flow over the wing. Under the vortex a secondary shock induced separation can be observed. And at high angles of attack and Mach numbers around 0.8 and above, vortex breakdown shows some aspects similar to shock induced separation. These examples illustrate the importance of shock induced separation at transonic conditions.

Contents

(24 pages in total)

"The only barrier is bad aerodynamics and bad planning"
Jack Ridley, X-1 Test Engineer

1 Introduction

"On October 5 (1947), I made my sixth powered flight and experienced shock-wave buffeting for the first time when I reached .86 Mach. It felt like I was driving on bad shock absorbers over uneven paving stones. The right wing suddenly got heavy and began to drop, and when I tried to correct it my controls were sluggish." These are the words from Chuck Yeager (1985), first to break the sound barrier. The phenomena he described are buffeting, wing rock and wing drop and essentially related to shock induced boundary layer separation, typical for the transonic flight regime.

Figure 1 serves as an appropriate starting point for this contribution. It shows the pressure distribution of the BELL X-1 measured in flight. The flow over the upper part of the airfoil is accellerated till locally supersonic speeds. At the rear of the airfoil a shock is formed followed by a pressure rise to return to free stream conditions. In the context of this paper flows with a locally supersonic region embedded in subsonic flow are called transonic. The shock that terminates this region interacts with the boundary layer on the airfoil surface and this interaction might cause separation of the boundary layer, shock induced separation, the theme of this contribution. The figure also shows a comparison with the pressure distribution measured in the wind tunnel. In this case the agreement is quite reasonable, but this is not necessarily always the case. The field of shock induced boundary layer separation will be criss-crossed, bringing together some observations of earlier work by the author on transonic wing development, delta wing flows and Reynolds number effects.

2 Two shocking experiences

Around 1950 Helen Gamble and Barry Haines (Haines, 1997) were testing on a Saturday afternoon an airfoil in the 10'x7' tunnel in Farnborough. The aim of the test was to study the effect of increasing the Reynolds number for an airfoil with free transition. The pressure distributions (fig. 2a) showed a clear shock wave. Some loss of suction could be seen just in front of the shock, the extent of which diminished with increasing Reynolds number. As expected, a gradual increase in lift coefficient was observed. However, when the boundary layer on the airfoil was made turbulent by applying a roughness band at 8 % chord (fig. 2b), the boundary layer was found to separate over the rear of the airfoil as indicated by the change in trailing edge pressure. The result was a significant loss of lift accompanied by a large change in pitching moment. This was quite an astonishing result, since it was well known that laminar boundary layers are much more apt to separate then turbulent boundary layers. Based on this, the belief was that transition fixation was the way to get a high Reynolds number answer and that Reynolds number effects were always favourable. It was quickly noted by Helen Gamble (1952) that the unexpected separation had to do with a different behaviour of the turbulent shock wave boundary layer interaction as compared with the laminar case.

In 1966 a NASA report written by Loving (1966) was published showing large differences between windtunnel and flight data for the C-141 aircraft (fig. 3). The story went around that for that reason the estimated pitching moment was completely wrong and the aircraft had to be trimmed by installing additional weight in the tail. Loving was much more reserved as he wrote: "the purpose of the discussion is to caution experimenters concerning the use of windtunnel results in predicting flight loads and moments when supercritical separated flow is present". Nevertheless figure 3 formed a familiar logo for subsequent reports advocating the need to build high Reynolds number windtunnels.

The observation of large differences in pressure distributions due to a change in Reynolds number was not limited to windtunnel flight comparisons. In 1980 NASA (McKinney, 1980) reported on F-111 flight tests that indicated a large variation in pressure distribution over the wing leading edge when the Reynolds number was doubled (fig. 4). These and similar examples have very much contributed to stories and worries about Reynolds number effects in aircraft design.

3 The art of modelling shockwave boundary layer interaction

Since the observations in the fifties, the difference between a laminar and a turbulent shock wave boundary layer interaction (fig. 5) is well understood in a qualitative sense. It is due to the fact that the velocity profile of a turbulent boundary layer is much "fuller" as compared with a laminar boundary layer. Consequently, the position of the sonic line in the laminar boundary layer is at about 1/3 of the boundary layer height as compared with the order of 1/10 for the turbulent case. Through this "subsonic corridor" between the sonic line and the wall the high pressure downstream of shock can communicate to the upstream flow in front of the shock. This upstream interaction thickens the boundary layer upstream of the shock. The thicker boundary layer turns the upstream supersonic flow through a number of compression waves, weakening the lower part of the shock and resulting in the typical lambda pattern. The pressure rise over the shock causes a local separation of the boundary layer that reattaches, partly under influence of transition in the laminar flow. The upstream interaction length and its decreasing scale at higher Reynolds numbers due to the thinning of the boundary layer, can clearly be seen in figure 2.

In most practical flows over aircraft, the Reynolds number is such that the boundary layer will be turbulent ahead of the shock. Hence turbulent shock wave boundary layer interaction has the most practical interest. For the turbulent case the situation is also quite complex (fig. 6). Due to the fact that the "subsonic corridor" is limited to a small region close to the wall, the upstream influence is more confined. The pressure rise underneath the shock results in a thickening of the boundary layer causing, at a higher shock Mach number (incipient) separation. When the Mach number is furher increased, the separation grows. As is the case with the laminar boundary layer, the separated flow reattaches. However, at a sufficiently high shock Mach number and depending on the downstream conditions, the flow might also fail to reattach resulting in a very thick separated boundary layer up till the trailing edge. This is illustrated in figure 7. In fact, figure 7 shows schematically two situations that might occur. Situation (a) named "type A separation" after Pearcey (1968) shows an expanding separation bubble underneath the shock. With increasing Mach number or incidence the separation will increase till the bubble reaches the trailing edge of the airfoil. When this occurs, the overall circulation around the airfoil is effected causing a loss of lift: this is called flow breakdown, a phenomenon related to buffet, maximum lift or lift divergence. Flow breakdown might also be reached in a different way, named "type B separation". The upstream shock wave boundary layer interaction has an adverse effect on the subsequent boundary layer development and promotes separation in the trailing edge region. This might occur when the pressure gradient over the rear of the airfoil is sufficiently strong. In that case the flow separates both under the shock and at the trailing edge. When the two separations merge, flow breakdown occurs. "Type B" separation is quite common on modern airfoils and in particular at tunnel Reynolds numbers. At higher Reynolds numbers the separation might

change from "type B" to "type A". Unfortunately, "type B" separation and its effects are (still) difficult to predict.

A detailed calculation of shock wave boundary layer interaction that describes all features shown in figure 6 and 7 is still beyond the state of the art. For routine calculations over airfoils and wings a boundary layer or a (thin layer) Navier Stokes formulation is fairly adequate to describe the effects for weak shocks. However, with separation under the shock and/or at the trailing edge, the results are less accurate and empirical relations are sometimes used to determine the effects of separation. Figure 8 shows as a typical example the Mach number for incipient separation (Stanewsky, 1981). A weak dependence on Reynolds number should be noted. This can be understood: the interaction is pressure dominated and viscous effects are of secundary importance.

More important for the prediction of flow breakdown is the work by Fulker and Ashill (1983) of DRA. They correlated for a large number of airfoils and wings the separation length (made dimensionless with the upstream momentum thickness) with the shock Mach number (fig. 9). Again, a rather weak dependence on Reynolds number (also based on the upsteam momentum thickness) can be observed, at least for the higher Reynolds numbers (the fall-off in separation length at low Reynolds numbers has to do with a typical low Reynolds number effect on boundary layers). The separation length appears to be a strong function of the shock Mach number. This correlation, entirely based on local conditions, is used to predict the buffet boundary: when the length of the separation bubble reaches the aft part of the airfoil where the steep gradient till the trailing edge pressure starts, the flow fails to reattach and flow breakdown will take place. Increasing the Reynolds number will have a strong effect on the separation length since the upstream momentum thickness decreases with increasing Reynolds number. Hence, the length of the separation bubble will decrease with increasing Reynolds number and flow breakdown will be postponed. Almost at the same time a more simple correlation was derived by the present author as depicted in figure 10. In this correlation the shock upstream Mach number at flow breakdown is directly correlated with the momentum thickness ahead of the shock, made dimensionless with the local chord. This purely empirical correlation, that is based on observations for a number of airfoils and wings, cannot be explained: why should the airfoil chord be of importance rather than local variables? Nevertheless, the correlation worked remarkable well and was incorporated in design codes.

4 (Mis)-Understanding Reynolds number effects

The airfoil or wing characteristics are conveniently summarized in the so called Lift-Mach number plane (fig. 11). It indicates the different flow regimes of the flight envelope. The two "sonic lines", one for the upper surface, the other for the lower surface, mark the points where the flow becomes locally supersonic. Beyond these lines the supersonic regions expand and shock waves will be formed. At the drag divergence boundary the drag suddenly starts to rise due to a rapid increase in shock strength. When the shock strength increases further shock induced separation and flow breakdown occurs, giving rise to the buffet or maximum lift boundary (C_L increasing) or the lift divergence boundary (Mach number increasing). At moderate Mach numbers there is a shock close to the leading edge of the airfoil that is the cause of flow breakdown. At higher Mach numbers the shock moves aft, limited by separation that causes the shock to move upstream again. From the pressure distribution follows the shock strength and the boundary layer conditions at the foot of the shock, in combination with the Reynolds number and the transition location. These parameters determine primarily flow breakdown and the off-design boundaries. In the design process, these boundaries are still primarily determined in the windtunnel and it is of considerable practical importance to know how they change with Reynolds number.

Reynolds number effects are the result of an interaction between the non-viscous outer flow and the viscous shear layer close to the airfoil or wing surface. Figure 12 gives a schematic representation of this interaction. As discussed above, the state of the boundary layer, either laminar or turbulent is of crucial importance. Also the possible interaction between shock induced and trailing edge separation was mentioned. All these effects determine the (viscous) conditions at the trailing edge and these in turn determine the overall lift and circulation.

For the evaluation of Reynolds number effects it is convenient to make a distinction between direct Reynolds number effects, related to all viscous effects at a fixed or "frozen" pressure distribution, depending directly on Reynolds number (like boundary layer transition, skin friction drag, separation) and indirect effects that show up as a variation in pressure distribution (e.g. variation in shock strength and/or position). Reynolds number effects are most systematically evaluated at constant lift as illustrated in figure 13. The airfoil drag has been plotted as a function of Reynolds number, either at constant lift (left) or at constant angle of attack (right). At constant lift a regular decrease in airfoil drag is obeserved whereas the evaluation at constant α indicates a not very systematic variation. The explanation can be found in the corresponding pressure distributions (fig. 14). We first look at the development at constant α. At the lowest Reynolds number of 3.6 million, there is a clear trailing edge separation, causing increased drag. This separation reduces the overall circulation and hence the lift, the strength of the shock and the shock wave drag. With increasing Reynolds number the shock strength increases and the separation decreases. The net effect on drag happens to be just opposite for $\alpha = 0^o$ and $\alpha = 1.3^o$.

However, at constant lift, the lift loss due to trailing edge separation has to be compensated by an increase in incidence. This causes a higher velocity level at the upper surface and increases the shock strength, resulting in higher drag. In this case the extra drag due to the shock wave and the separation act in the same sense. This explains the regular variation of drag with Reynolds number for all lift values. In a more general way one can state that at constant lift an increase in Reynolds number will result in a re-distribution of lift over the airfoil in such a way that the lift is shifted from the nose to the trailing edge, resulting in a more negative pitching moment.

In figure 15 typical pressure distributions measured on the C-141 wing are plotted together with windtunnel results for the NLR airfoil 7301. The left side of this figure shows hardly any variation in pressure distribution with increasing Reynolds number whereas the right side indicates large and somewhat similar effects. The explanation is that in the latter case the pressure distributions represent conditions just around the separation boundary. At higher Reynolds numbers the separation disappears and this causes large changes in pressure distribution. One should not be puzzled by these large variations but accept this as being an essential characteristic of the variation across a discontinuity. Instead, one should evaluate the variation of the discontinuity itself. This is illustrated in figure 16 where the maximum lift boundary is plotted as a function of Reynolds number. A very regular behaviour is found in line with the simple models of shock wave boundary layer interaction discussed above. The figure is also a good illustration of the favourable effect of laminar shock wave boundary layer interaction especially at higher Mach numbers when the shock is more downstream. These and similar examples illustrate that Reynolds number effects can be understood in a qualitative way if the analysis is made in the right way as indicated schematically in figure 17.

Finally one should be aware of an important difference between the separation illustrated in figure 14 and the one indicated in figure 15. In the former case, the airfoil is well within the boundary for flow breakdown and "massive" separation has not yet occurred. This, "type B" separation is critically important for the prediction of drag near the cruise condition, where advanced airfoils might show signs of trailing edge separation at tunnel Reynolds numbers. When the Reynolds number is sufficiently large, the trailing edge separation will disappear and the flow becomes rather unsensitive to a Reynolds number change. However, on the right side of figure 15 one is close to or beyond flow breakdown. Flow breakdown will also be observed at higher Reynolds numbers, as indicated by the continuous and systematic trend of the maximum lift boundary in figure 16.

This does not mean that Reynolds number effects are fully understood in a quantitative sense. To predict how much the drag value decreases and the separation boundary improves between windtunnel and flight, is still a difficult question. Of course, with high Reynolds number windtunnels like the NTF of NASA and the ETW in Europe, the flight Reynolds number can be duplicated in the windtunnel. Pressurized windtunnels, like the HST of NLR, have the possibility to change the Reynolds number during a test such that trends with Reynolds number

can be measured. In fact, much of the experience with Reynolds number effects of the author resulted from these type of studies at NLR (Elsenaar, 1988). The so observed trends can be compared with theoretical predictions to support an extrapolation procedure. Care should be taken to fix the boundary layer transition to eliminate unwanted transition point variations and laminar shock wave boundary layer interactions that have a large effect on drag and the separation boundaries.

Another technique for estimating full scale behaviour exploits the effect of boundary layer thickness on separation development as presented in figure 9 and 10. When the boundary layer in front of the shock is laminar at tunnel Reynolds numbers, so called "aft fixation" can be used to reduce the boundary layer thickness in front of the shock. The question then is what criterion should be used to determine the boundary layer trip position. The most simple criterion one can think of states that to simulate high Reynolds number characteristics, the transition should be fixed such that the boundary layer thickness at the trailing edge of a flat plate at the tunnel Reynolds number is the same as in flight for forward transition. This so called "zero level simulation criterion" (see Elsenaar in Laster, 1988), that incidently has some relation with the well known form factor method for drag prediction, is shown in figure 18. A much more refined approach is to match the length of the shock induced separation bubble for windtunnel and flight using the correlation presented by Fulker and Ashill as shown in figure 9. An example is given in figure 19. With this technique it is possible indeed to simulate the flight pressure distributions in the windtunnel. The pros and cons of the various techniques are discussed in more detail by Laster (1988).

5 Shock induced leading edge separation on delta wings: an airfoil point of view

The discussion so far was concerned with (almost) two-dimensional flows on airfoils or high aspect ratio wings as used on transport type aircraft. These wings are designed for minimum drag and attached flow at the cruise condition. At higher lift coefficients or Mach numbers the shock on the wing increases in strength causing shock induced separation, typically just outboard of the kink region (fig. 20). The wing is swept to allow flight at higher Mach numbers to postpone separation: the Mach number component perpendicular to the shock determines the shock wave strength.

Delta wings for fighter aircraft are designed for high manouvrability in combat action. This requires sustained lift even at high incidences at the expense of higher drag values. The lift at higher incidences results from a strong vortex above the wing (fig. 21). The vortex is formed at the highly swept leading edge due to separation of the boundary layer. At low free stream Mach numbers the separation is due to the steep pressure peak at the leading edge. Is it likely that shock induced separation will occur at higher Mach numbers?

To study the flow development at the leading edge, the Mach number component, $Mach_N$, in a plane perpendicular to the leading edge is important. This can easily be understood from the "infinite swept wing analogy" (fig. 22b & c). In the absence of viscosity is the flow over a swept (sweep angle Λ^o) and a two-dimensional airfoil identical when the Mach number perpendicular to the leading edge $M_\infty.\cos\Lambda$ is identical (note that the flow on a two-dimensional airfoil in a windtunnel will not change when the model is pulled with a speed $M_\infty.\sin\Lambda$ through the tunnel). This analogy can be used to study the flow in the leading edge region of the delta wing (fig. 22a). Of course this analogy only holds in the vicinity of the leading edge. Also the effective incidence at the leading edge of the delta wing cannot be carried over to the infinite swept wing case due to the different geometry and spanwise load distribution (induced incidence). Nonwithstanding these restrictions, the analogy can be used to explain typical transonic characteristics of the leading edge separation in a qualitative sense. Figure 23 shows pressure distributions (full lines) derived from the infinite swept wing analogy using full potential inviscid 2-D calculations. These calculations are made for increasing incidence at a free stream Mach number of .4 and .85 (for the delta wing) respectively. At the lower Mach number a pressure peak develops at the wing leading edge. The pressures measured on the wing surface (symbols) follow the calculated values quite well (note lack of resolution in the leading edge region). The steep pressure gradient in the nose region causes the boundary layer to separate as observed in the experiment between 10 and 12^o and resulting in the start of a vortex as is evident from the pressure peak that is formed at 94 % half-span (it is of interest to compare this with fig. 4). At the higher free stream Mach number of .85 the calculations show a typical transonic development of the pressure distribution with a plateau region terminated by a shock that moves

downstream. Note that the free stream Mach number in a direction perpendicular to the leading edge ($Mach_{\infty,N}$) is only .36 in this case but the local Mach numbers are clearly supersonic. The shock strength increases rapidly with α and exceeds a value of the order of 1.5 required for shock induced separation. Hence it is likely that at this Mach number of .85 shock induced separation is the cause of vortex formation. This process can further be illustrated with figure 25 that shows a surface oilflow pattern for this 65 deg delta wing at Mach=.85 (Elsenaar, 1988). At a location of 15 % of the root chord, the separation bubble under the shock breaks up and forms an open separation with vortex formation. The dark line is most likely the shock. Between the leading edge and this shock attached flow can be seen.

This explanation is further supported with the results of similar infinite swept wing calculations at higher free stream Mach numbers. Figure 24 indicates the shock position (distance from the nose) for a range of free stream Mach numbers. Note that in all these cases the leading edge is still "subsonic" (free stream Mach number normal to the leading edge Mach $_{\infty,N} < 1$). The figure shows at a free stream Mach number ($Mach_{\infty}$) between 1.2 and 1.7 a rapid downstream movement of the shock. This is supported by oil flow pictures. At $Mach_{\infty}$=.85 (shock induced) separation starts almost right at the leading edge (fig. 25) but at $Mach_{\infty}$=1.7 the flow remains attached over a larger region near the leading edge (fig. 26). In this region the flow can still be regarded as quasi two-dimensional (slow variation along the leading edge) and the infinite swept wing analogy might still hold locally. At a still higher free stream Mach number of 2.2, the leading edge becomes "supersonic", the shock has moved further inboard and is now clearly conical (fig. 27). These simple arguments help to explain in a qualitative sense the flow development with increasing Mach number and the formation of a shock that causes the separation and vortex formation.

6 More shocks in the flow field: separation underneath the vortex and up in the air

Apart from a small region around the leading edge where the infinite swept wing analogy might be applied for certain conditions, the flow over a delta wing with a vortex present is highly three-dimensional (fig. 21). Are there other shocks in the flow field. And if so, do they cause separation? For the infinite swept wing analogy we have seen that the Mach number perpendicular to the leading edge determines the occurence of a shock and its strength. Since all isobar planes are parallel to the leading edge, this can be generalised intuitively as follows: for the occurence of shocks in the flow field it is necessary that the local Mach number component in a direction perpendicular to the local isobar plane is larger than 1.

This seems to be the case for at least two regions in the flow field. In figure 28 the isobars on the wing surface for a free stream Mach number less than 1 are depicted schematically. When the vortex is formed, the flow over the larger part of the wing is conical. At the rear of the wing the isobars will be symmetrical around the plane of symmetry and locally parallel to the trailing edge. From this sketch two regions can be spotted where the local Mach number might become larger than 1 in a direction perpendicular to the local isobar plane: underneath the vortex and near the trailing edge in the symmetry plane (fig. 28).

Figure 29 shows the surface streamlines for the condition Mach=.85, $\alpha=20^{o}$. The topology of the flow is such that an attachment line is present at the symmetry plane. Moving outward from the symmetry plane, the surface streamlines are more and more curved untill they appear to run into a straight line that has a white area of accumulated oil further outside. From the measured pressure distribution (fig. 30) and assuming conical flow, the local Mach number and the flow direction can be calculated. From this, the cross-flow Mach number, that is the Mach number component in a direction perpendicular to a conical ray (the direction of the local isobar) can be derived. The result of this calculation, made by Houtman (1988) of Delft University is presented in figure 312. The figure clearly indicates that the cross-flow Mach number exceeds a value of 1 and will be strong enough to force separation at an incidence of about 20^{o}. Hence the sharp line in figure 29 indicates a local shock, followed by a shock induced separation. The occurence of such a cross flow shock underneath the vortex has been reported by other authors (e.g. Wendt, 1983) and the presented analysis provides another argument for its existence.

An other region where shocks might occur can be found over the rear of the wing. When the Mach number and/or the incidence increases, the flow in the symmetry plane of the wing will become supersonic (fig. 32). Near the trailing edge the flow has to return to subsonic conditions. The local Mach number component is also in this case perpendicular to the local isobar (fig. 28) and a shock will be formed to match the downstream free stream conditions. This shock is clearly visible in the high quality schlieren pictures made by Donohoe (1996) using the (flat) wing surface as a mirror (fig. 33, 34). The pictures give some evidence of the cross flow shocks

underneath the vortex as discussed above. Of particular importance here is the shock wave at about 80 % root chord. When the incidence is increased from 22^o to 24^o this single shock suddenly transforms into a double shock system. It appears that this change is coupled to the breakdown of the vortices above the wing. Vortex breakdown has been explained in different ways and is still debated (see e.g. Délery, 1994). But it is well known that when a vortex moves into a region with an adverse pressure gradient, vortex breakdown will occur if the pressure rise is sufficiently strong. The explanation of vortex breakdown in that case is very similar to the separation of a boundary layer. Due to viscous effects resulting from the high shear stresses (in case of a boundary layer near the wall, for a vortex in the vortex core) a loss of total pressure will occur. When the adverse pressure gradient is sufficiently strong, the (reduced) momentum of the flow can no longer cope with the pressure gradient and locally reversed flow will result. If this is the case for boundary layer flow, separation occurs and the boundary layer experiences at the separation point a very rapid increase in thickness. This is also observed for vortex breakdown. Figure 35 shows the rapid increase in the cross sectional area of the vortex as observed with laser sheet visualization by Bütefisch (Elsenaar, 1988). Is the shock the cause of the vortex breakdown? It is most likely that both the shock and the vortex breakdown are the result of the existence of a pressure gradient over the rear of the delta wing and consequently an essential transonic flow phenomenon.

This type of vortex breakdown can have very severe implications for transonic flight at yawed conditions as illustrated with figure 36. In this figure the rolling moment is presented for various incidences as a function of the yaw angle β. At a Mach number of .85 the rolling moment shows a sudden jump that is caused by a-symmetric (on one of the wing halves) vortex breakdown. If Chuck Yeager had flown this configuration he certainly would have complained about wing drop. It is one more illustration that in transonic flow, shocks in combination with separation like phenomena, may give rise to sudden discontinuïties and surprises.

Acknowledgements

This review is based on work done at NLR in close co-operation with Fokker and, for the delta wing flow, as part of the Joint International Vortex Flow Experiment. I would like to thank my colleagues at NLR, Fokker and the Technical University of Delft for all stimulating discussions. The Fluid Dynamics panel of AGARD has provided the international forum where the results of most of these studies could be presented and discussed with others. In that respect I would like to mention in particular Barry Haines, Pat Ashill and Egon Stanewsky.

7 References

1. Délery, J., 1994 - Aspects of Vortex Breakdown. *Progress in Aerospace Sciences, 30:1-59*

2. Donohoe, Sharon R., 1996 - Vortex Flow and Vortex Breakdown above a Delta Wing in High Subsonic Flow: an experimental investigation. *Dissertation, Technical University Delft*

3. Elsenaar, A. Bütefisch, K.A., 1988 - Experimental Study on Vortex and Shock Wave Development on a 65◦ Delta Wing. *IUTAM Symposium Transonicum III, Göttingen*

4. Elsenaar, A. et al, 1988 - The International Vortex Flow Experiment. *AGARD CP 437 "Validation of computational fluid dynamics", paper 9*

5. Elsenaar, A. 1988 - Observed Reynolds Number Effects on Airfoils and High Aspect Ratio Wings at Transonic Flow Conditions. *NLR MP 88006U. Also part of AGARDograph 303 on "Reynolds Number Effects in Transonic Flow"*

6. Fulker, J.L., Ashill, P.R. 1983 - A study of the factors influencing shock-induced separation on swept wings. *RAE TR 83088*

7. Gamble, H.E. 1952 - Some effects of Reynolds number on a cambered wing at high subsonic Mach numbers. *ARC CP 105*

8. Haines, A.B., Holder, D.W. and Pearcy, H.H. 1957 - Scale effects at high subsonic and transonic speeds, and methods for fixing boundary layer transition in model experiments. *ARC R&M 3012*

9. Haines, A.B. 1987 - Scale Effects in Transonic Flow. *27th Lanchester Memorial Lecture. Aeronautical Journal August/September 1987*

10. Haines, A.B. 1997 - private communication

11. Houtman, B. 1988 - private communication

12. Laster, M.L. 1988 - Boundary Layer Simulation and Control in Windtunnels. *Report of the Fluid Dynamics Panel Working Group 09. AGARD Advisory Report No.224*

13. Loving, D.L. 1966 - Wind Tunnel Flight Correlations of Shock Induced Separated Flow. *NASA TN D-3580*

14. McKinney, L.W., Baals, D.D. 1980 - High Reynolds Number Research. *NASA Conference Publication 2183*

15. Pearcey, H.H., Osborne, J., Haines, A.B. 1968 - The Interaction Between Local Effects at the Shock and Rear Separation - A Source of Significant Scale Effects in Wind-Tunnel Tests on Airfoils and Wings. *AGARD CP 35, paper 11*

16. Seddon, J. 1967 - The flow produced by interaction of a turbulent boundary layer with a normal shock wave of strength sufficient to cause separation. *ARC R&M 3502*

17. Stanewsky, E. 1981 - Interaction between the outer inviscid flow and the boundary layer on transonic airfoils. *Dissertation, TU-Berlin, D 83*

18. Wendt, J.F., Vorropoulos, G. 1983 - Laser Velocimetry Study of Compressibility Effects on the Flow Field of a Delta Wing. *AGARD CP 342, Paper 9*

19. Yeager, Chuck. 1985 - Yeager, an autobiography. *Bantam Books*

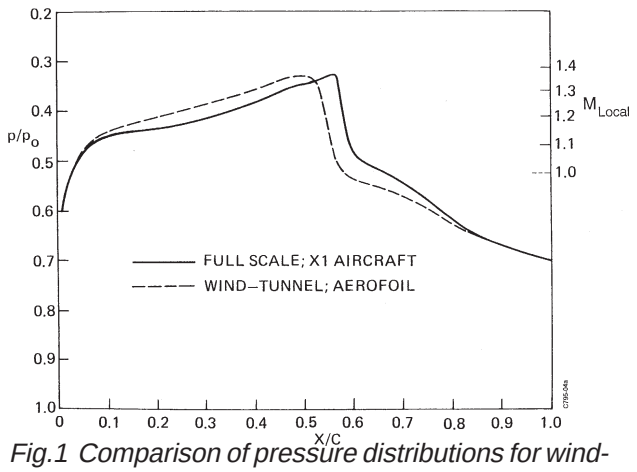

Fig.1 Comparison of pressure distributions for wind-tunnel and flight for the Bell X-1 Aircraft (Pearcey, 1968)

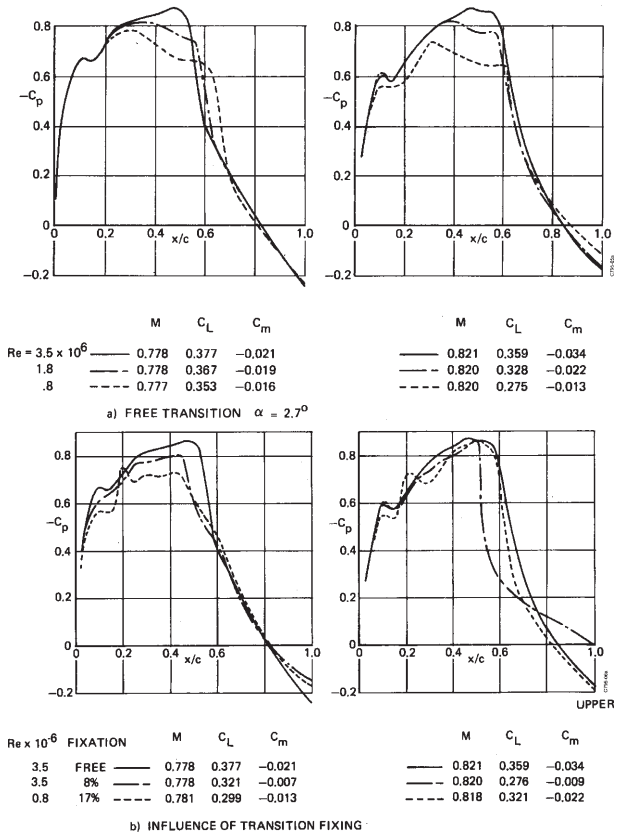

Fig.2 Early evidence of the effect of Reynolds number and transition fixation on the pressure distribution (Gamble, 1952)

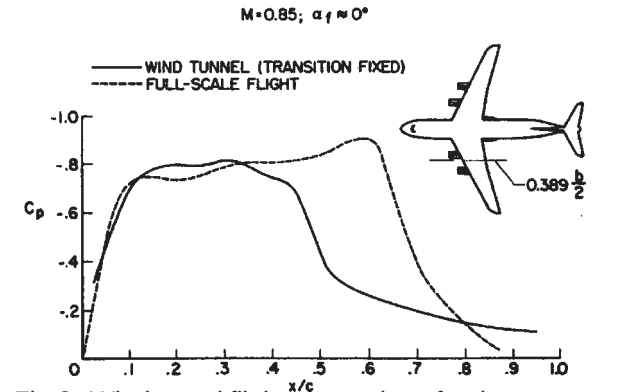

Fig.3 Windtunnel flight comparison for the C-141 aircraft (Loving, 1966)

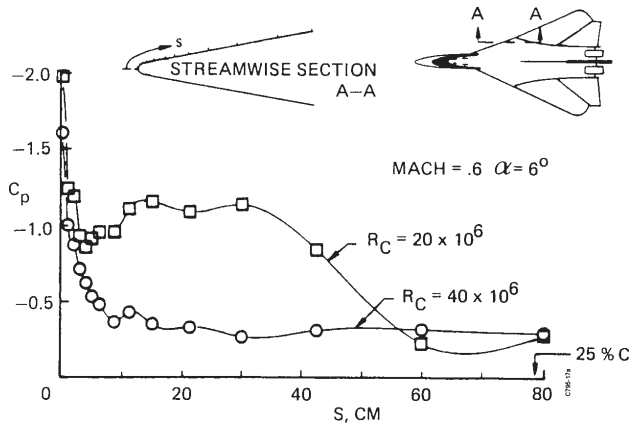

Fig.4 Reynolds number effect on the pressure distribution close to the leading edge of a delta wing at vortex formation (McKinney, 1980)

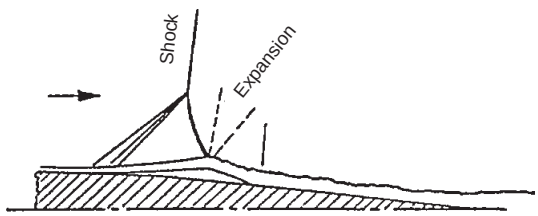

(a) Laminar boundary layer

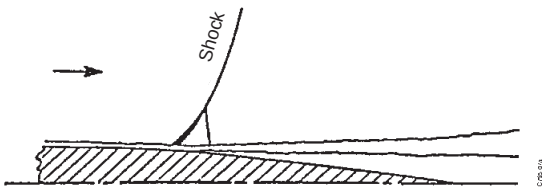

(b) Turbulent boundary layer

Fig.5 Flow patterns for laminar and turbulent separated boundary layer interaction (Haines, 1957)

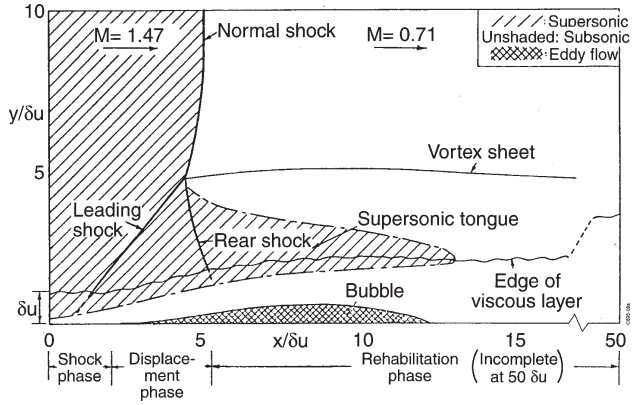

Fig.6 The interaction of a normal shock with a turbulent boundary layer (Seddon, 1967)

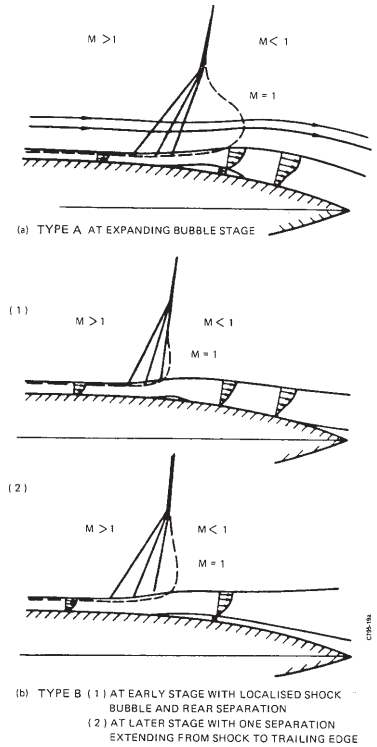

Fig.7 "Type A" and "type B" separation (Pearcey, 1968)

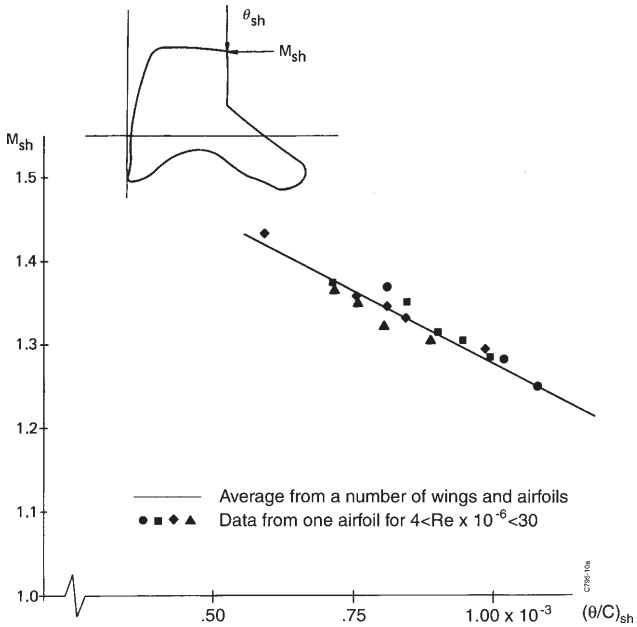

Fig.10 A simple correlation for the buffet onset boundary (Elsenaar, unpublished)

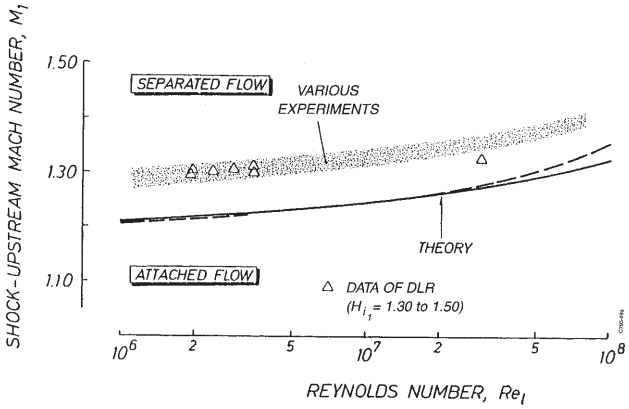

Fig.8 Reynolds number dependence of incipient separation (Stanewsky, 1981)

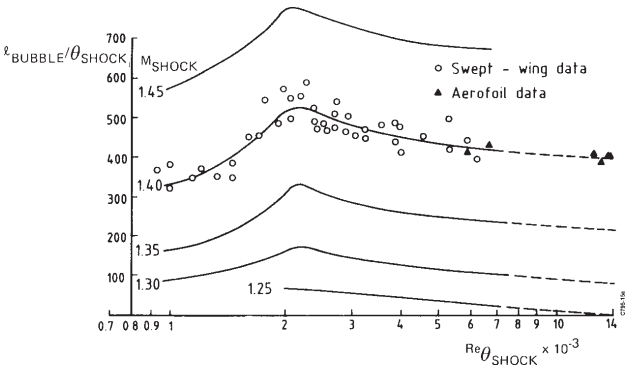

Fig.9 Correlation for the length of the separation bubble underneath a shock (Fulker, 1983)

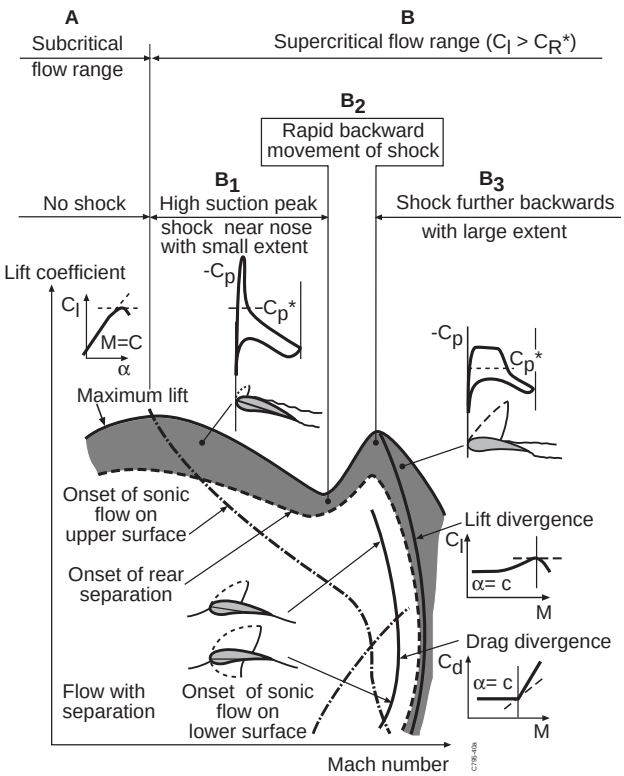

Fig.11 Airfoil characteristics in the C_L-Mach number plane

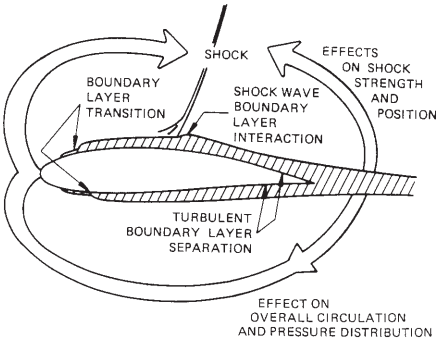

DOMINANT RE-NUMBER EFFECT		
CHARACTERISTIC	DIRECT	INDIRECT
LIFT AND PITCHING MOMENT		X
VISCOUS DRAG	X	
WAVE DRAG		X
DRAG DIVERGENCE		X
BOUNDARY LAYER SEPARATION	X	
BUFFET BOUNDARY	X	X

Fig.12 Schematic representation of direct and indirect Reynolds number effects (Elsenaar, 1988)

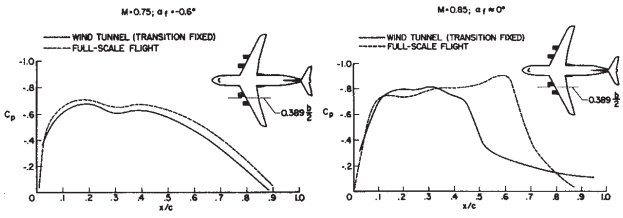

a) C141 Windtunnel / flight comparison

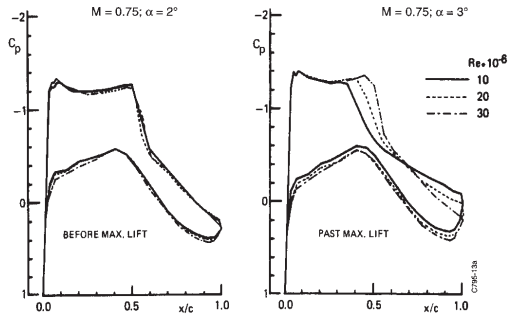

b) High Reynolds number windtunnel tests of 2-D airfoil

Fig.15 Illustration of large variations in pressure distribution close to the separation boundary

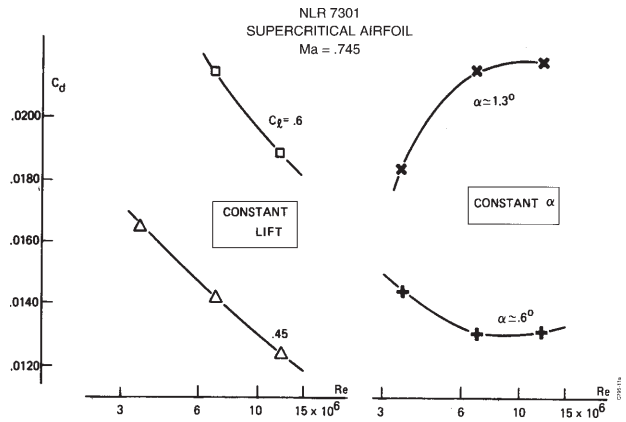

Fig.13 Illustration of Reynolds number effects at constant lift or constant incidence (Elsenaar, 1988)

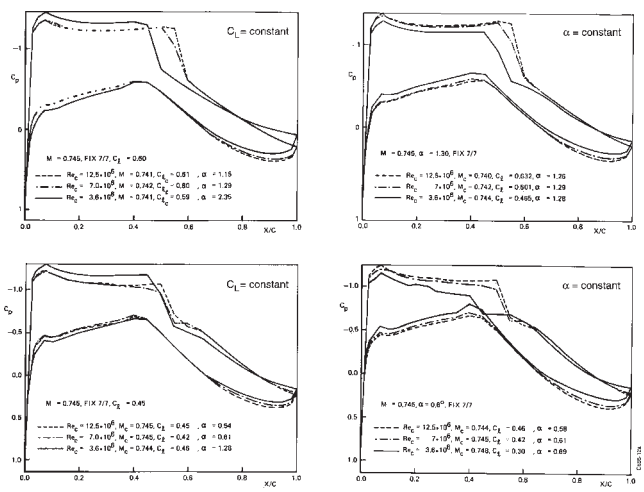

Fig.14 Pressure distributions corresponding to figure 13

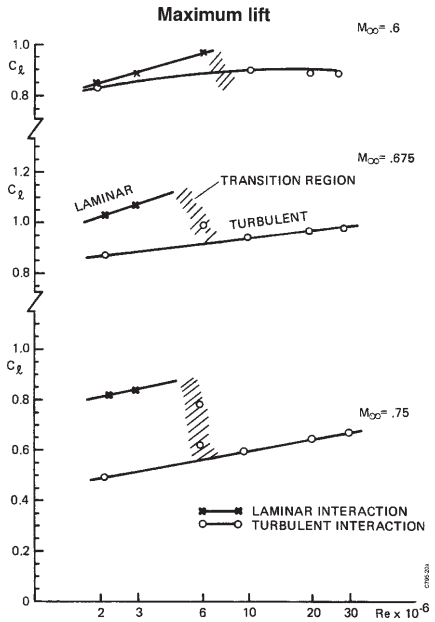

Fig.16 Variation of maximum lift with Reynolds number for laminar and turbulent flow (Elsenaar, 1988)

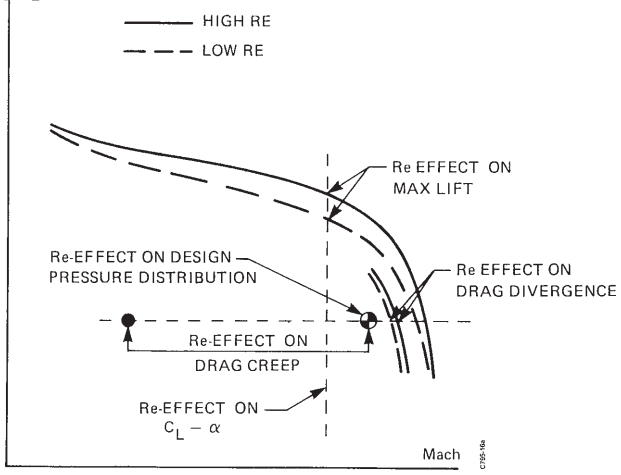

Fig.17 The evaluation of Reynolds number effects in the C_L-Mach number plane (Elsenaar, 1988)

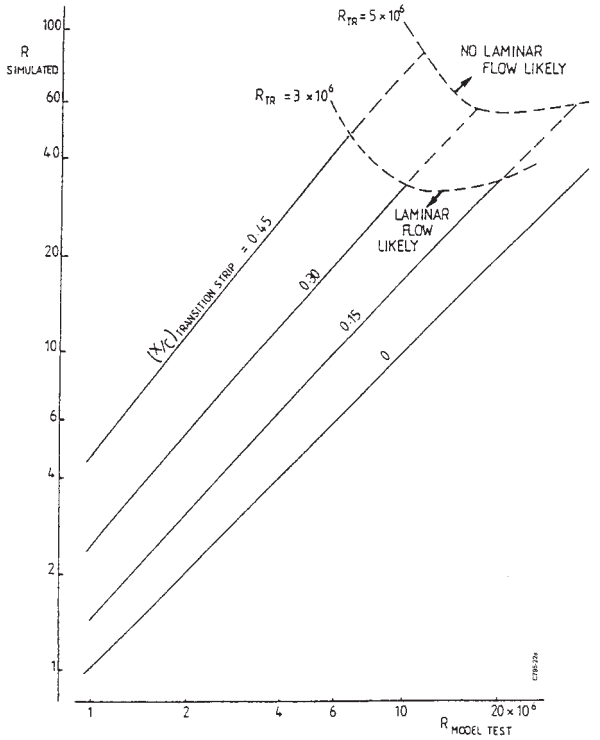

Fig.18 The "Zero level simulation criterion" for high Reynolds number simulation (in Laster, 1988)

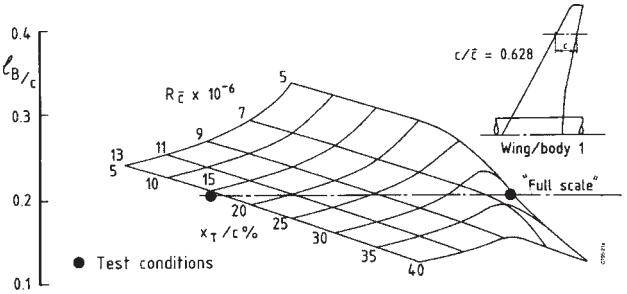

Fig.19 A more advanced simulation cerion based on figure 9 (Mach = .78, C_L = .7) (Fulker, 1983)

Typical transport aircraft wing shock pattern
(buffet onset at design Mach number)

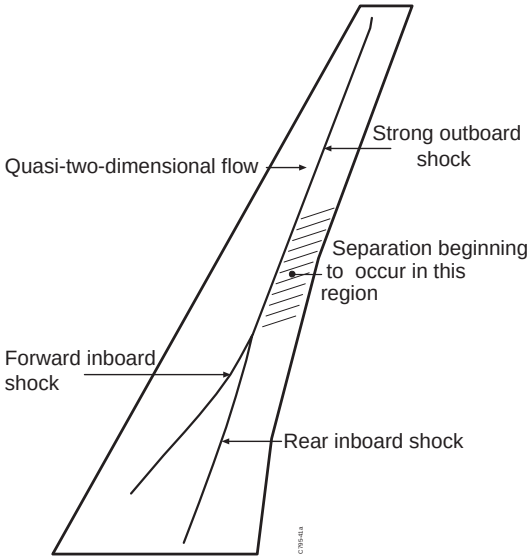

Fig.20 Shock wave formation on a transport type wing near the buffet boundary (in Laster, 1988)

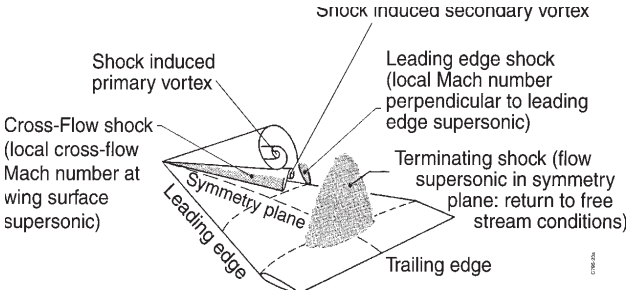

Fig.21 Shock wave formation on a delta wing, tentative (Elsenaar, 1988)

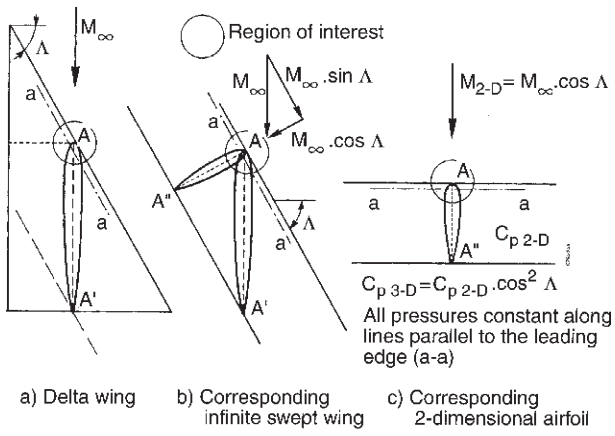

Fig.22 The infinite swept wing analogy applied to leading edge flow (Elsenaar, 1988)

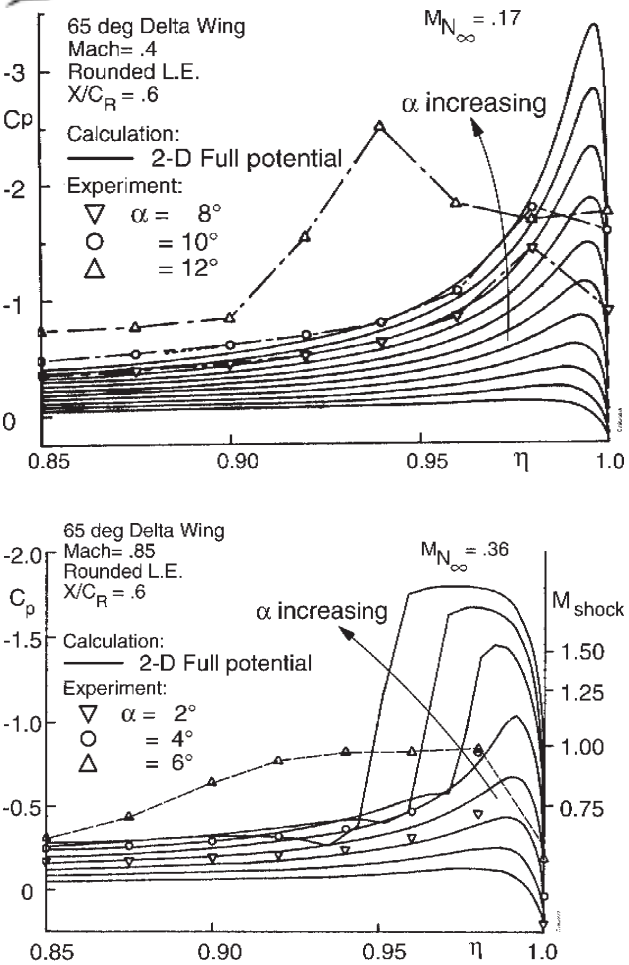

Fig.23 The development of the pressure distribution at the leading edge for a 65 deg delta wing as calculated from the infinite swept wing analogy (Elsenaar, 1988)

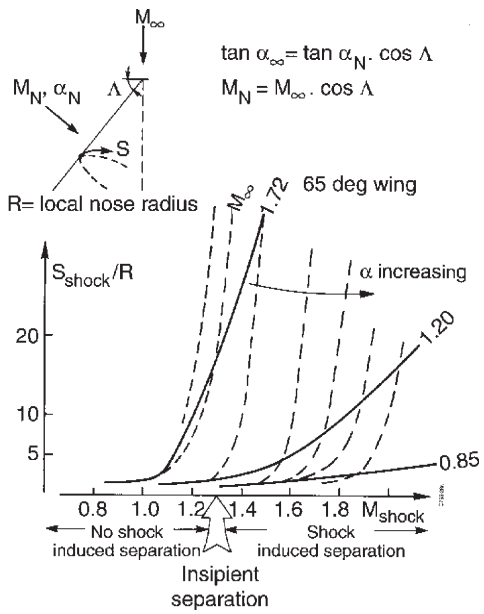

Fig.24 Shock wave position as a function of shock wave strength as calculated from the infinite swept wing analogy (Elsenaar, 1988)

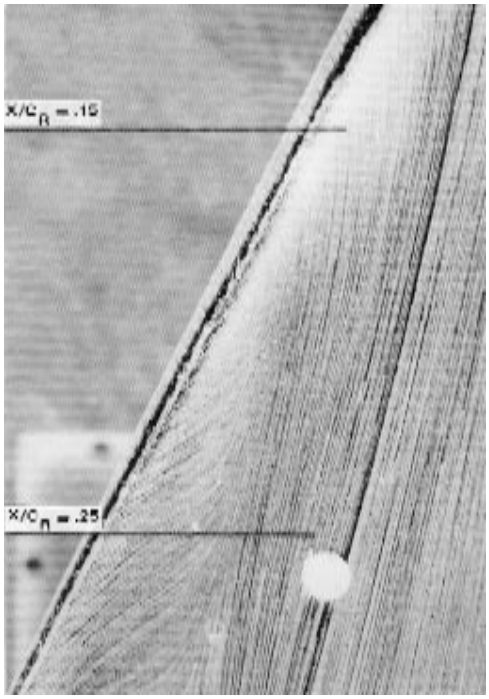

Fig.25 Detail of leading edge flow showing vortex formation; 65 deg delta wing with rounded leading edge, Mach=.85, α=10 degrees (Elsenaar, 1988)

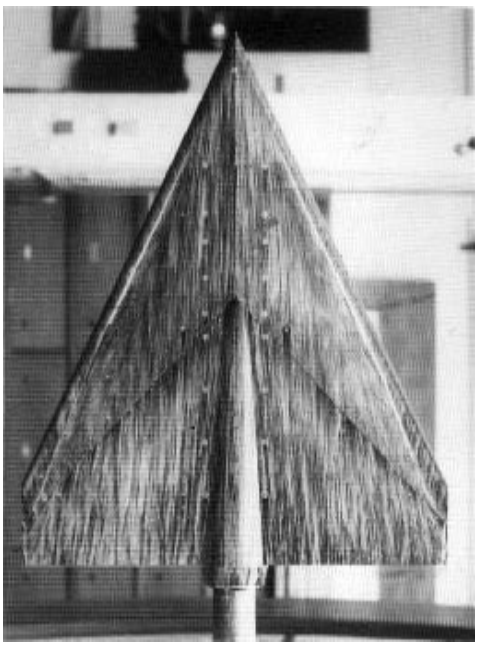

Fig.26 Oil flow visualization indicating attached flow close to the leading edge followed by shock induced primary separation and vortex formation; subsonic leading edge, 65 deg delta wing with rounded leading edge, Mach= 1.72, α= 4 degrees (Elsenaar, 1988)

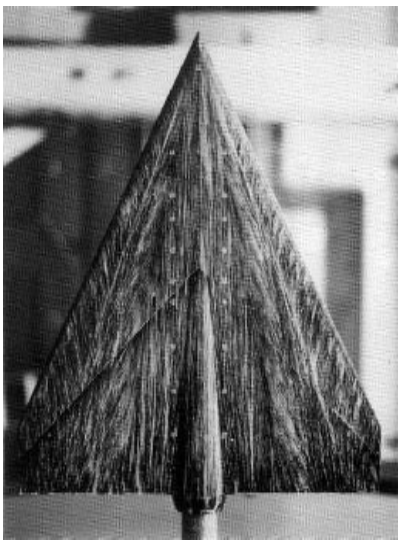

Fig.27 Oil flow visualization indicating attached conical flow close to the leading edge followed by shock induced separation and vortex formation; supersonic leading edge, 65 deg delta wing with rounded leading edge, Mach= 2.18, α= 8 degrees (Elsenaar, 1988)

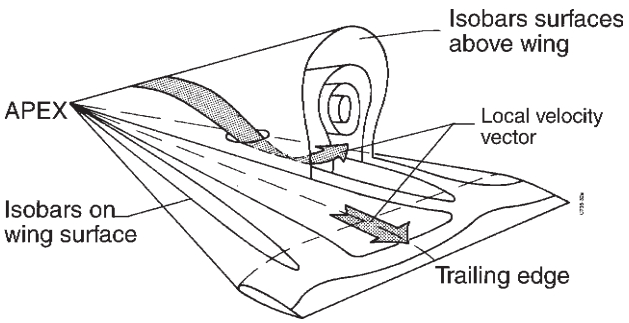

Fig.28 Isobar surfaces on a delta wing at transonic conditions - tentative (Elsenaar, 1988)

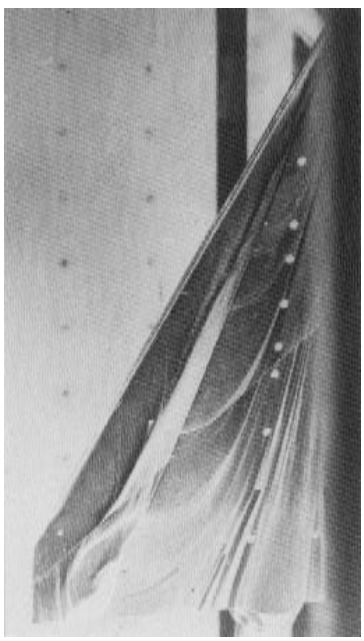

Fig.29 Detail of oil flow visualization indicating shock induced secondary separation; 65 deg delta wing with rounded leading edge, Mach=.85, α=20 degrees (Elsenaar, 1988)

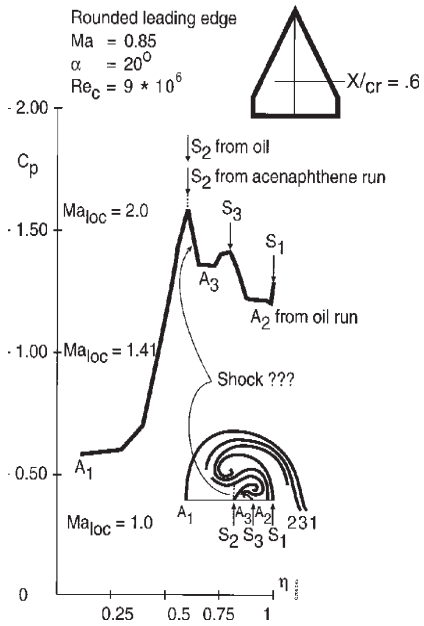

Fig.30 Spanwise pressure distribution (X/C_R=.6) corresponding with figure 29 (Elsenaar, 1988)

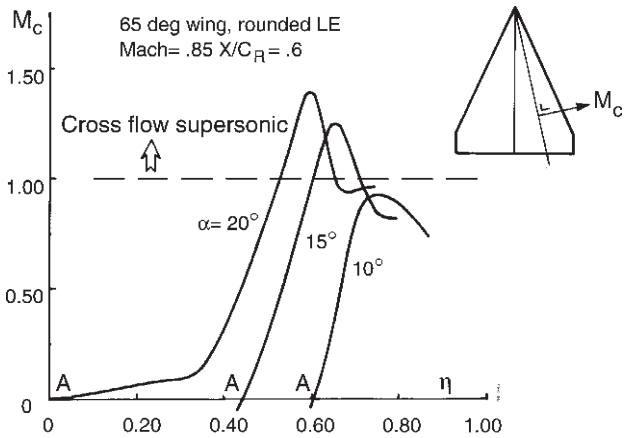

Fig.31 Calculated cross flow Mach numbers on the surface calculated from the pressure distribution shown in figure 30 (Houtman, 1988)

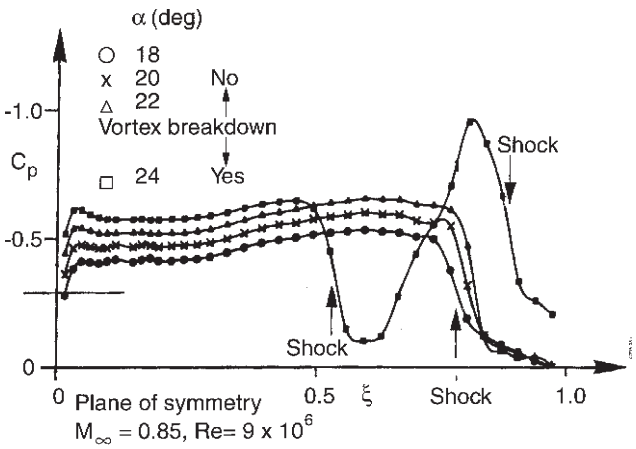

Fig.32 Pressure distributions in the symmetry plane of a 65 deg delta wing indicating shock wave development and related vortex breakdown at Mach=.85 (Elsenaar, 1988)

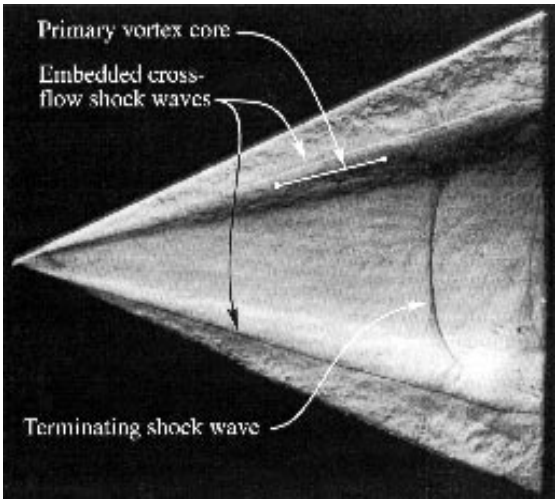

SRV Image M_∞ = .8 α = 15°

Fig.33 Surface Reflection Visualization on a 65° delta wing showing shock wave formation before vortex breakdown at Mach=.80, α=15° (Donohoe, 1996)

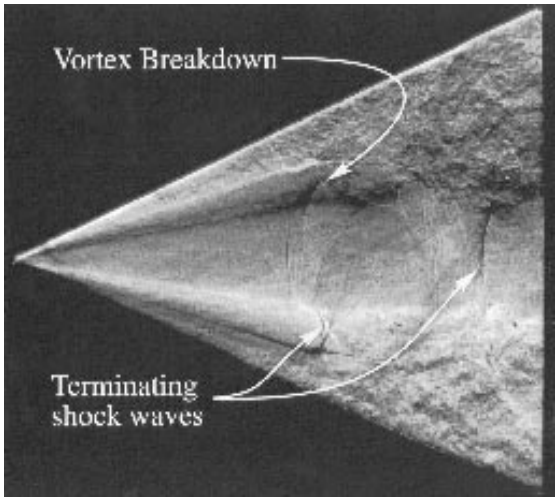

SRV Image M_∞ = .8 α = 25°

Fig.34 Surface Reflection Visualization on a 65° delta wing showing shock wave formation after vortex breakdown at Mach=.80, α=20° (Donohoe, 1996)

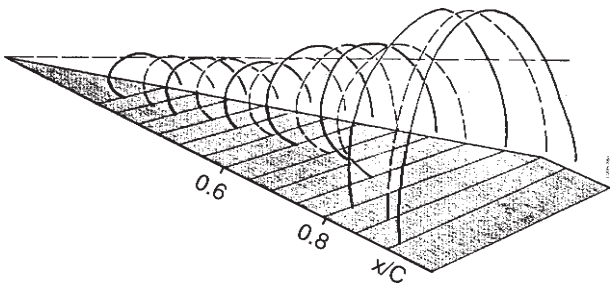

Fig.35 Cross sectional aerea of the vortex showing rapid growth due to vortex breakdown; laser sheet visualization by Bütefisch, DLR (Elsenaar, 1988)

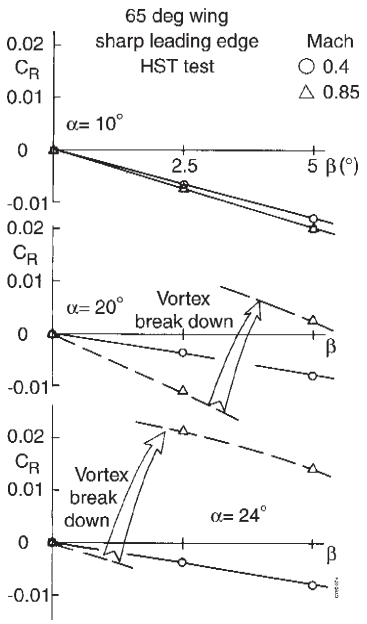

Fig.36 Discontinuities in rolling moment due to vortex breakdown at yawed conditions; 65 deg delta wing, sharp leading edge (Elsenaar, 1988)